TAYLOR-COUETTE FLUID FLOW WITH FORCE OSCILLATION IN THE INNER-CYLINDER USING THE IMMERSED BOUNDARY METHOD

Jonatas Emmanuel Borges, jonataseb@yahoo.com.br
Marcos Antonio de Souza Lourenço, lourenco@mecanica.ufu.br
Elie Luis Martinez Padilla, epadilla@mecanica.ufu.br
Aristeu da Silveira Neto, aristeus@mecanica.ufu.br
Federal University of Uberlândia – 2121 João Naves de Ávila, Av – Campus Santa Mônica

Andre Martins Leibsohn, aleibsohn@petrobras.com
CENPES/Petrobras

Abstract. *As new challenges arise in the exploration of deep and ultra-deep water oilfields by Petrobras, more knowledge and research are needed, so that tools could be developed to assist in the critical operations and make things practicable. In the context of the drilling process, the complexity of the fluid flow inside the riser is associated with the nature of the non-Newtonian flow, immersed solid particles, variable eccentricity and the superimposed traveling azimuthal waves on the inflow and outflow boundaries of the Taylor vortices. This work presents the numerical three-dimensional results of the following simplified fluid flows: Taylor-Couette, Taylor-Couette with varying imposed eccentricity and Taylor-Couette with forced oscillation in the inner cylinder. Using the Navier-Stokes equations, a finite volume method discretization with second order accuracy in both time and space was utilized to simulate the Newtonian, single-phase incompressible fluid flow in the three cases. The circular walls of the inner and outer cylinders are represented by the immersed boundary method, with the direct multi-forcing model. The determined results allow to evidence the flow structures in the three cases in a very qualitative way, even so in the presence of the inner cylinder oscillation.*

Keywords: *immersed boundary method; Taylor-Couette fluid flow; incompressible flow; oscillation in the inner-cylinder; finite volume method.*

1. INTRODUCTION

The deep water production systems consist of different risers applied for production, drilling, workover, export, etc. In recent years, the knowledge and development of tools for optimization of these processes has received significant attention from the scientific community. The drilling process could be simplified as the fluid flow occurring in the annulus of two concentric cylinders, named Taylor-Couette. Although very studied, the Taylor-Couette flow with added forced inner-cylinder rotation and translation has only a few references and experimental data in the literature.

In 1923 Taylor published groundbreaking observations of the flow states in this system, which we refer to today as the Taylor-Couette system Taylor (1923), and have allowed to create a stability flow map, although the first investigations was made by Couette (1890) and Mallock (1896). In the Taylor-Couette flow there is a centrifugal instability resulting from the rotation of an inner cylinder relative to a concentric outer cylinder. In the simplest and the most practical case where the outer cylinder is fixed, at high enough speed of rotation of the inner cylinder, centrifugal forces overcome the viscous forces and donut shaped toroidal vortices fill the space between the cylinders. However, with forced translation of the inner cylinder, a different dynamic is presented in the whole flow. With the spatial oscillation of the inner cylinder, the vortices are no more symmetric, becoming thin in the region where the inner cylinder is near the outer cylinder wall and thick in the opposite region to ensure mass conservation.

There is much experimental and numerical work concerning about the particularities mentioned above. Although a variety of experimental techniques have been used to acquire spatial and temporal data for time-dependent Taylor-Couette flow (Wereley and Lueptow, 1994), most of these suffer from significant drawbacks such as providing only single velocity component data. Others techniques, like PIV appear capable of providing space and time resolved multi-component velocity data in more than a single spatial dimension. On the other hand, in the recent years, the advance of the computation power and numerical algorithms, have allowed the so called *numerical experimentation* (Ferziger and Peric, 1999); (Piomelli and Balaras 2002), resulting in simulations with good agreements with experimental data (Padilla *et al.*, 2009); (Hwang and Yang, 2004).

Cylindrical, unstructured and orthogonal computational meshes are usually utilized for the discretization of the annulus between cylinders. The immersed boundary method is a computational cheap alternative to represent the boundaries of a geometrically complex body while using a Cartesian mesh as the Eulerian domain (Peskin, 1977). Some elaborated models of immersed boundary are the *physical virtual model* of Silva et al. (2003) and, more recently, the *multi-direct forcing* of Wang et al. (2007).

2. MATHEMATICAL AND NUMERICAL MODELLING

A fluid isothermal and incompressible, with constant physical properties was considered. The computational modelling is built upon the mass continuity and Navier-Stokes equations that in dimensional form and Cartesian coordinates are respectively presented as:

$$\frac{\partial u_i}{\partial x_i} = 0 \tag{1}$$

$$\frac{\partial u_i}{\partial t} + \frac{\partial (u_i u_j)}{\partial x_j} = -\frac{1}{\rho}\frac{\partial p}{\partial x_i} + \nu\frac{\partial^2 u_i}{\partial x_j \partial x_j} + \frac{f_i}{\rho} \tag{2}$$

were u_i and p are the velocity components and pressure field respectively, ρ is the density and ν is the kinematic viscosity. The source term f_i include the Eulerian force due the immersed boundary contribution to represent the immersed bodies in the flow. The force field representation are made in a mathematical manner using the auxiliary function Dirac delta $\delta(x)$ in Eq. (3).

$$\vec{f}(\vec{x},t) = \int_\Gamma \vec{F}(\vec{x}_k,t)\,\delta(\vec{x}-\vec{x}_k)\,d\vec{x}_k \tag{3}$$

where the k denotes a Lagrangian variable and $\vec{F}(\vec{x}_k,t)$ is the Lagrangian force, determined in the points of the solid interface. The Fig. (1) shows the Lagrangian and Eulerian domains representation in yellow and green respectively.
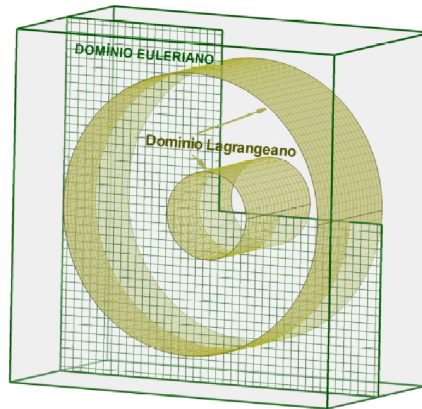

Figure 1: Eulerian and Lagrangian domains representation.

The Lagrangian force is determined using the *multi-direct forcing method* proposed by Wang *et al.* (2007). The model dynamically estimate the fluid force on the solid surface of the body immersed in the flow. Adding the temporal parameter u^* to Eq. (2) give:

$$\frac{u_i^* - u_i^t}{\partial \Delta t} + \frac{\partial (u_i u_j)}{\partial x_j} = -\frac{1}{\rho}\frac{\partial p}{\partial x_i} + \nu\frac{\partial^2 u_i}{\partial x_j \partial x_j} + \frac{f_i}{\rho} \tag{4}$$

It could be seen here that u^* is a mathematical term satisfying the momentum conservation equation. Now the Lagrangian force can be calculated as:

$$\frac{F_k}{\rho} = \frac{u_k - u_i^*}{\Delta t} \tag{5}$$

Determined the force F_k, it is distributed across the Eulerian points around the index k using Eq. (3). In this paper, the discretization of the governing equations Eqs. (1-5), for the eulerian field use the finite volume method (Patankar, 1980) in a staggered computational mesh, using the schemes Adams-Bashforth in time and central-differences in space, both of second order. The velocity pressure coupling uses a two step fractional step method of Kim and Moin (1985) with the *Strongly Implicit Procedure* SIP (Stone, 1968) as the Poisson pressure correction solver.

3. PROBLEM DESCRIPTION

Here are presented three cases of the Taylor-Couette flow: normal, with forced oscillation and with variable eccentricity. In the first two cases the flow development occur in the annulus with constant gap between the cylinders and are illustrated in Fig. (2a), with the exception that the second case has forced oscillation of the inner cylinder in axial direction. The third problem has the flow development in the annulus between the outer and the eccentric inner cylinder, depicted in Fig. (2b). In the three cases the inner cylinder has angular velocity ω, regarding with his geometrical center, and the outer cylinder are stationary.

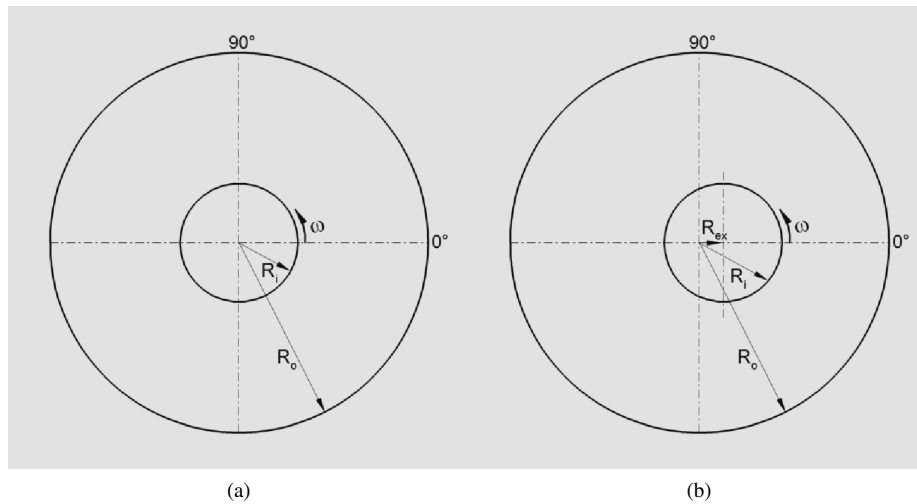(a)   (b)

Figure 2: Two-dimensional illustration of the studied cases of the Taylor-Couette flow; (a) concentric cylinders and (b) inner cylinder with eccentricity.

In Fig. (2), R_o and R_i are the extern and internal cylinders radius and R_{ec} is the eccentricity radius. Additionally, the channel has length L in the axial direction, gap $E = R_o - R_i$, eccentric velocity ω_{ec}, and the following non-dimensional parameters: radius ratio $R = \frac{R_o}{R_i}$, aspect ratio $A = \frac{L}{R_o}$ and the Taylor number $Ta = \frac{\omega R_i E}{\nu}$. In the axial direction boundaries was adopted the boundary condition of periodicity.

4. Results

The simulations were realized using a Lagrangian domain defined by $R_i = 0.125$ m, $R = 3.2$ and $A = 1$ and the Eulerian domain by $A \times A \times 0.6A$. The computational mesh is structured and non-regular with 106000 volumes in Eulerian portion and 3360 cells for the outer cylinder and 1056 for the inner cylinder representation in the Lagrangian section.

4.1 Taylor-Couette

According to Taylor (1923), who investigate experimentally and analytically flows between rotating concentric cylinders, for small gaps E between them (compared with the radii of the internal cylinder R_i), the problem simplifies and becomes dependent on the Taylor number Ta. When this parameter increases above the critical value, counter-rotating axisymmetric vortices of toroidal shape arises in the flow, also referred to as Taylor-Couette instabilities. Although in this case E is greater than R_i, the above criteria is applicable and, according Lueptow and Docter (1992), the critical Taylor number for $\frac{R_o}{R_i}$ is approximately $Ta = 65$.

The Taylor vortices arise naturally for $Ta = 100$ in steady state. In the cross sectioned slices of Figs. (3a and 3b) are depicted the u and v components of the velocity field respectively. Both figures show the velocity vector directions. The isosurface of the w velocity is given in Fig. (4) and show the Taylor vortices with wave length E. The natural wave length is $2E$, however the settings of the axial length of the computational domain L and the boundary conditions of periodicity force the occurrence smaller wave lengths. These results agree very well with the ones in the work of Padilla *et al.* (2007).
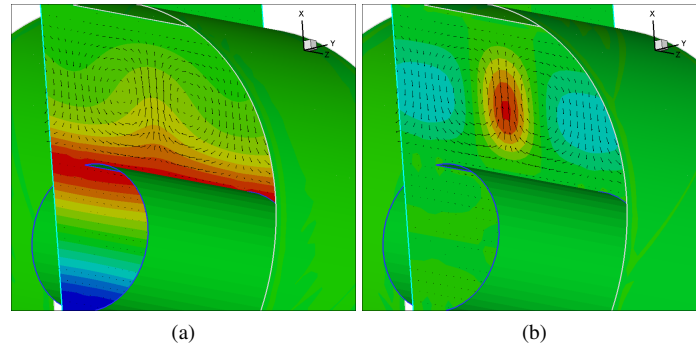
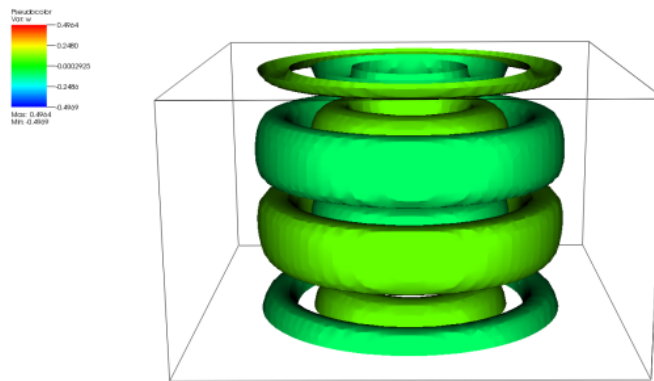Figure 3: Velocity field components; (a) u and (b) v.

Figure 4: Isosurface of the axial velocity component w.

4.2 Taylor-Couette with forced oscillation

The inner cylinder oscillate with the tangential velocity given by the expression of Eq. (6). The configuration is the same of the case without oscillation.

$$V_{tg} = \omega R_i = A_o \sin\left(2\pi f_c t\right) R_i \tag{6}$$

where A_o stands for the amplitude, f_c is the frequency and t is physical time, in accordance with He *et al.* (2000).

There is so little work on literature related to the effect of rotation and oscillation in Taylor-Couette flow, however for the two-dimensional case, Silva (2008) show some results of the fluid flow around blunt bodies. In this work the amplitude was adopted as 1% of the inner cylinder rotational velocity while varying the frequency. The velocity of rotation is calculated using the expression of the Taylor number $\omega = \frac{\nu Ta}{ER_i}$. The Fig. (5) presents the behavior of the velocity of rotation of the inner cylinder in time. The cases (a) through (c) represent the velocity using the Eq. (6) while in the case (d) we have the case without oscillation, with $\omega = 29.09 s^{-1}$. The frequencies for each case are: (a) $f_c = 0.463 s^{-1}$, (b) $f_c = 0.923 s^{-1}$ and (c) $f_c = 1.389 s^{-1}$.

Using a temporal probe in an intermediary position on the gap between the cylinders, in $z = \frac{L}{2}$, it can be seen the small frequencies more representative in the flow for the case with oscillation. In such case the variation is smaller than the great frequencies, that tend to case without oscillation, as depicted in Figs. (6), (7) and (8). It must be observed the small deviation values when compared with the velocity captured by the numerical probe.
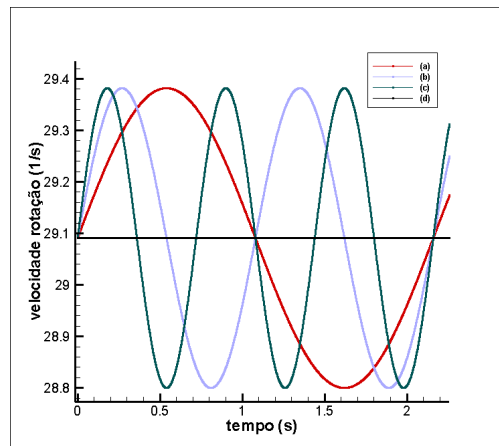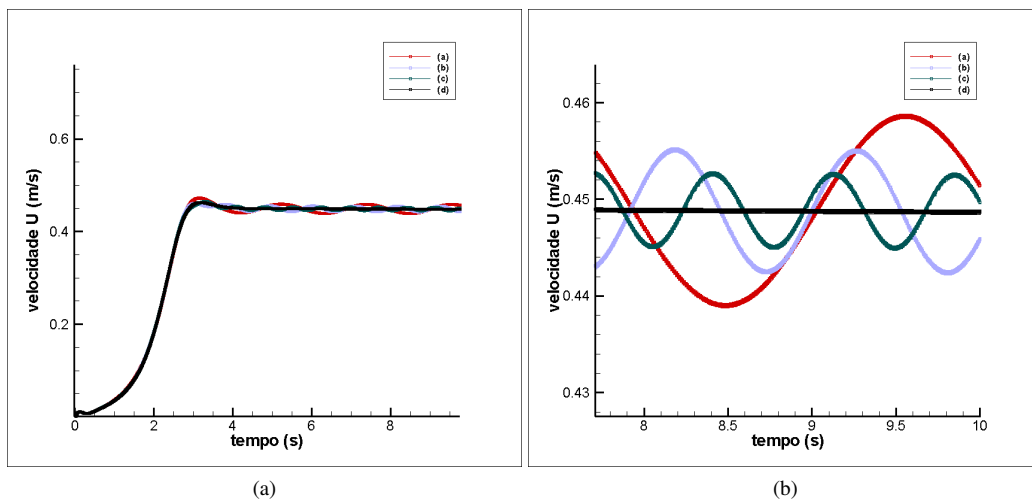
Figure 5: Velocity of rotation of cylinder ω.

(a)   (b)

Figure 6: Velocity u for the cases of rotation/oscillation captured using a temporal probe.

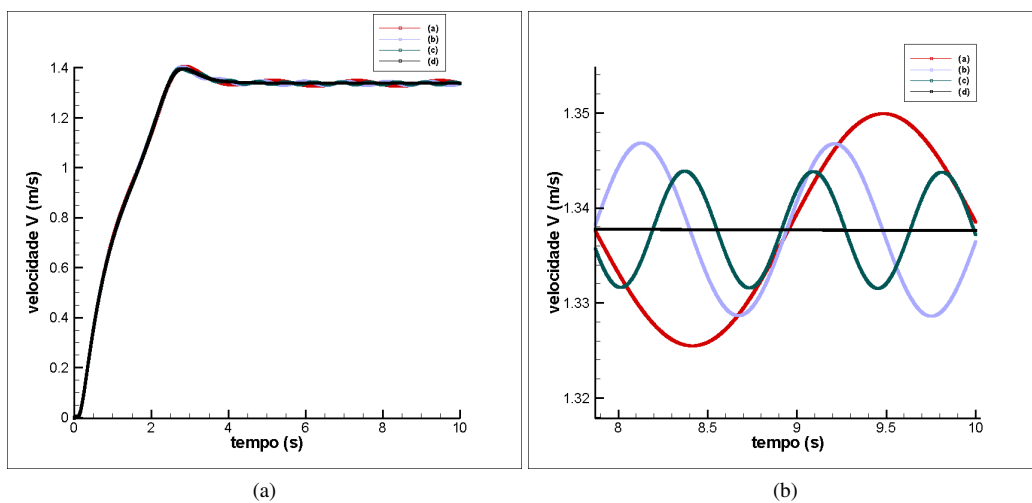(a)   (b)

Figure 7: Velocity v for the cases of rotation/oscillation captured using a temporal probe.
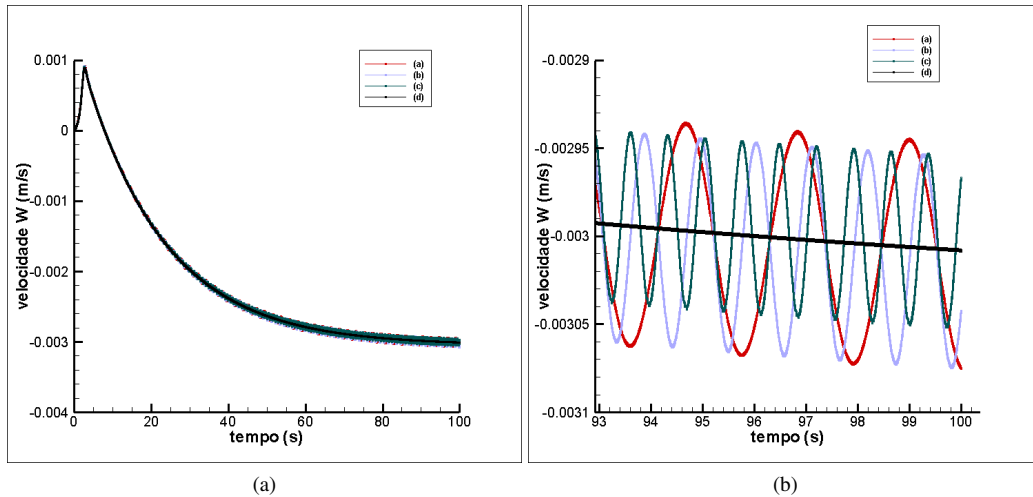
(a) (b)

Figure 8: Velocity w for the cases of rotation/oscillation captured using a temporal probe.

It can be seen in Figs. (6), (7) and (8) that all cases converge at same time to steady state. The thickness of the vortices is affected varying the velocity of rotation, as observed in Fig. (9) for the isosurfaces of $w = 0.1ms^{-1}$, respectively in $10.5s$ and 11.5 of simulation.
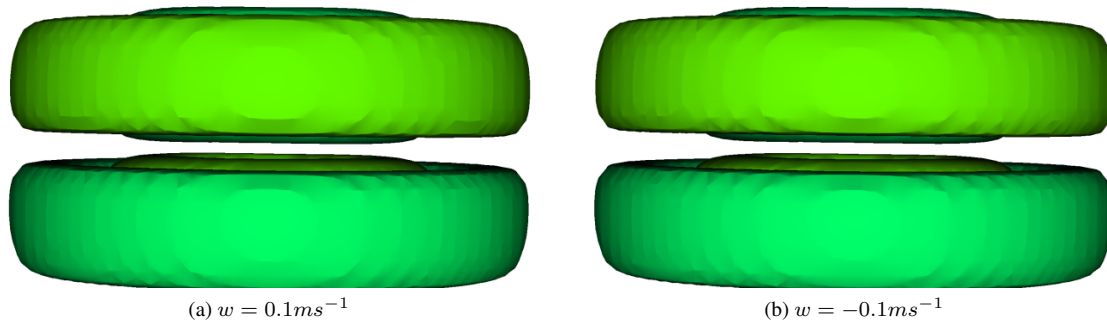

(a) $w = 0.1ms^{-1}$ (b) $w = -0.1ms^{-1}$

Figure 9: Isosufaces of velocity w.

4.3 TAYLOR-COUETTE WITH TRANSLATION OF THE INNER CYLINDER

In this section the case of translation of the inner cylinder in the axial direction is studied. Initially, the cylinder is considered to be at rest in the position $(0.6, 0.5, 0.3)m$ and initiates a cyclic movement around the center $(0.5, 0.5, 0.5)m$ at $\omega = 1s^{-1}$ and the geometry of cylinder can be seen in Fig. (10). The center position for each direction (x and y) can be visualized in Fig. (11).

Is possible to see that in the case with rotation and translation of the inner cylinder the different dynamic of the flow dislocate the steady state to a higher instant, as the vortices take more time to be fully developed. In this case was utilized $w = 0.01ms^{-1}$. In Fig. (12) is possible to see the thin vortices in positions where the inner cylinder lies next to the outer cylinder and thick structures in the other side, ensuring the mass conservation.

The profile at position $x = 0.6m$ and $z = 0.3m$ is only dependent of the y direction within the position $y = 0.5m$. Thus, this profile will be analyzed for the u and v velocity in the instant $20s$ and verify the behavior of the flow. In the case of u velocity, there is no alteration on the profile when compared with the classical Taylor-Couette, however there is small deviations over the inner cylinder surface. It should be due the translation movement in the z direction, so that velocities in the x and y presents the positive values $u = 0.005\frac{m}{s}$ and $v = 0.628\frac{m}{s}$ respectively. In the position $y = 0.375m$ we have $u = 3.636\frac{m}{s}$ and $v = 0\frac{m}{s}$ and in $y = 0.625m$ we have $u = -3.636\frac{m}{s}$ and $v = 0\frac{m}{s}$ in the faces of the inner cylinder for the case without translation. This characteristic symmetry cannot be visualized in the case with translation of the inner cylinder, like depicted in Fig. (13a). It occurs mainly because while the cylinder behave like a rigid body, the velocity of rotation is dependent of the relative position of the cylinder and the fluid next to the cylinder wall tends to acquire its velocity (Fig. 13a).
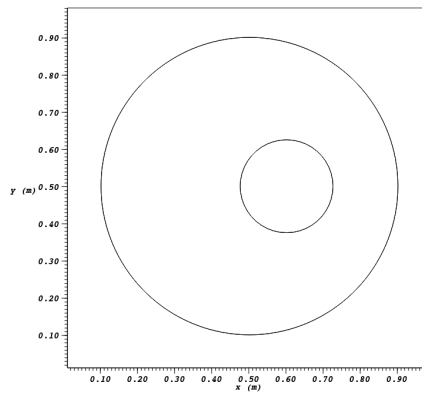
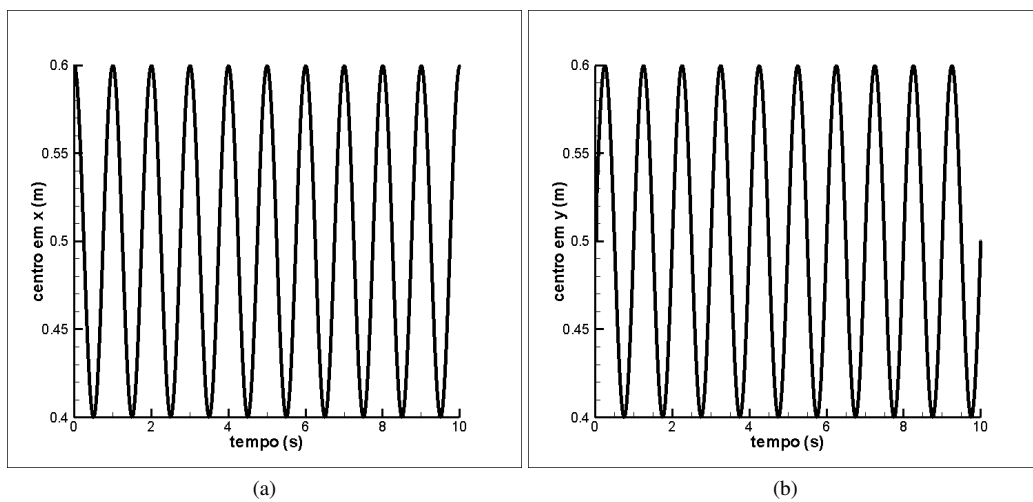Figure 10: Initial configuration of the cylinders in the beginning of simulation.

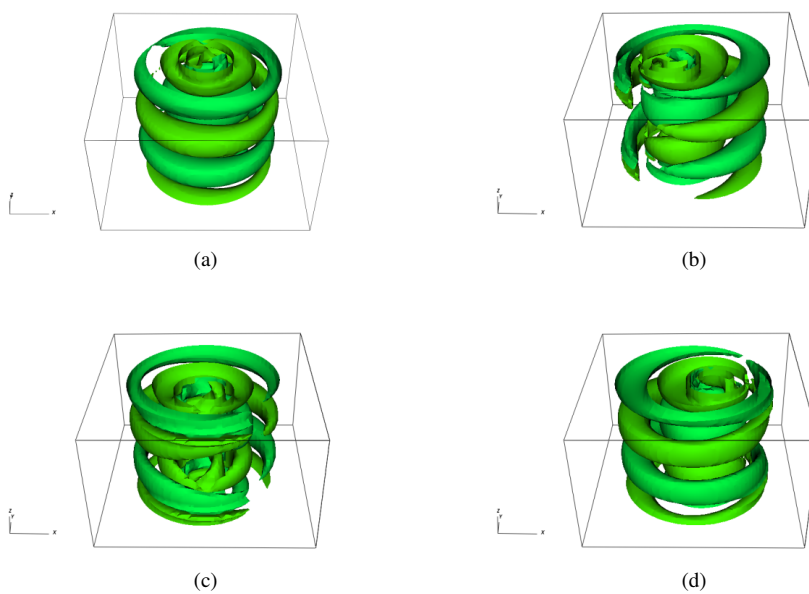Figure 11: Center position components during the simulation.

Figure 12: Fluid structures development during forced translation of the inner cylinder.
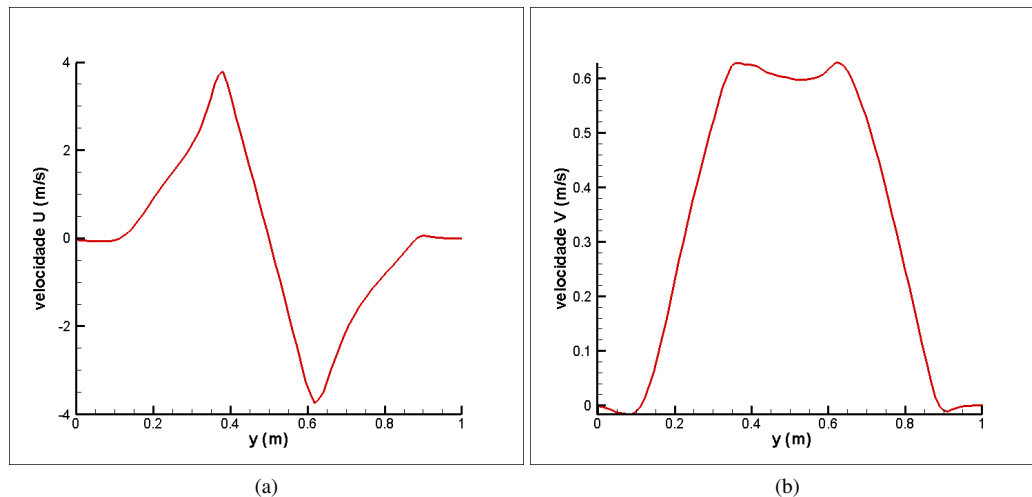
Figure 13: Velocity profiles for a point in the inner cylinder surface in the midplane of the flow; (a) velocity u and (b) velocity v.

5. CONCLUSION

In this work was presented a series of numerical results on simplified forms of the Taylor-Couette flow using the incompressible model of the Navier-Stokes equations and the immersed boundary method. The physical behavior observed in the results, like the Taylor-Couette instabilities, demonstrate the ability of the *multi-direct forcing method* in represent the rigid boundaries for the Taylor-Couette problem and the time spent in the simulations was very attractive, using the serial code. Even so, in order that be established, it is necessary a comparison with experimental data in a quantitative way, reminding that is a little number of experimental studies with the configuration presented in the present work.

6. ACKNOWLEDGEMENTS

7. REFERENCES

Couette, M. Couette, 1890, Etudes sur le frottement des liquides, Ann. Chim. Phys. 6, pp. 433–510.

Ferziger, J. H.; Peric, M., Computational methods for fluid dynamics, 2nd Ed., Springer, 1999.

Fogelson, A.L.; Peskin, C.S., A Fast Numerical Method for Solving the Three-dimensional Stokes' Equations in the Presence of Suspended Particles. Journal of Computational Physics, vol. 79, pp. 50-69, 1988

Goldstein, D.; Hadler, R.; Sirovich, L., Modeling a No-Slip Flow Boundary with an External Force Field. J. Comput. Physics, 105, pp. 354, 1993.

He, J. W.; Glowinsky, R.; Metcalfe, R.; Nordlander, A.; Periaux, J., 2000, "Active Control and Drag Optimization for Flow Past a Circular Cylinder I. Oscillatory cylinder Rotation", Journal of Computational Physics 163, 83-117.

Hwang J.; Yang K.; 2004, "Numerical study of Taylor-Couette flow with an axial flow", Computer and Fluids 33, 97–118.

Kim, J; D Moin, P., Application of a fractional step method to incompressible Navier-Stokes equations. J. Comp. Phys., 59, pp. 308-323, 1985.

Lima e Silva A.L.F., Silveira-Neto A; Damasceno, J.J.R., 2003, Numerical simulation of two-dimensional flows over a circular cylinder using the immersed boundary method. Journal of Computational Physics, 189, pp. 351–370.

Mallock, A.,1896, "Experiments on fluid viscosity", Philos. Trans. R. Soc. London, Ser. A 187, 41–56.

Mohd-Yusof, J., Combined Immersed Boundaries/B-Splines Methods for Simulations of Flows in Complex Geometries. CTR Annual Research Briefs, NASA. Ames/Stanford University, 1997

Padilla, E.L.M.; Lourenço, M.A.S.; Silveira-Neto, A., 2009, "3D numerical solver in cylindrical coordinates for incompressible flows: validation process". In: International Congress of Mechanical Engineering, 2009, Gramado-RS. 20th COBEM, p.171.

Padilla, E.L.M.; Martins, A.L.; Silveira-Neto, A., "Simulação numérica de escoamentos internos tridimensionais usando o método de fronteira imersa". In: Anais do Congresso Brasileiro de Engenharia e Ciências Térmicas. Curitiba, 2006a, vol. 1, pp. 1-8.

Padilla, E.L.M.; Martins, A.L.; Silveira-Neto, A., "Aplicação do método de fronteira imersa à tecnologia de perfuração em

águas profundas". In: Anais do Encontro Nacional de Hidráulica de Perfuração e Completação de Poços de Petróleo e Gás. Vitória-Pedra Azul, 2006b, vol. 1, pp. 1-7.

Padilla, E.L.M.; Martins, A.L.; Silveira-Neto, A., "Experimentação numérica sobre escoamentos em canais anulares". In: Congresso Brasileiro de Pesquisa e Desenvolvimento em Petróleo e Gás. Campinas, 2007.

Padilla, E.L.M.; "Aplicação de simulação numérica para análise de escoamentos transicionais em canais cilíndrico-anulares com excentricidade variável". Projeto de Pesquisa desenvolvida no Laboratório de Mecânica dos Fluidos da Faculdade de Engenharia Mecânica 2007.

Patankar, S.V., "Numerical Heat transfer and Fluid Flow. Hemisphere Publishing Corporation". New York, 1980.

Peskin, C. S., Numerical analysis of blood flow in the heart. Journal of Computational Physics, vol. 25, pp. 220-252, 1977.

Piomelli, U.; Balaras, E., Wall-Layer for Large-Eddy Simulations. Annu. Rev. Fluid Mech, vol. 23, pp. 349-374, 2002

Silva, A. S., "Modelagem Matemática de interação fluido-estrutura utilizando o método de fronteira imersa". Tese de doutorado do Programa de Pós Graduação em Engenharia Mecânica da Universidade Federal de Uberlândia 2008.

Stone, H.L., "Iterative Solution of Implicit Approximations of Multidimensional Partial Differential Equations". SIAMJ Numer. Anal., vol. 5, pp. 530-558. 1968.

Taylor, G.I. "Stability of a Viscous Liquid Countained Betwenn Two Rotatin Cylinders". Phil. Trans R Soc., vol. A223, pp. 289-343, 1923.

Uhlmann M. An immersed boundary method with direct forcing for the simulation of particulate flows. Journal of Computational Physics, New York, v. 209, p. 448-476, 2005.

Unverdi, S.O.; Tryggvason, G.A. "Front-Tracking Method for Viscous Incompressible Multi-Fluid Flows". J. Comput. Physics, 100, pp. 25-60, 1992.

Wereley, S.T.; Lueptow, R.M. "Azimutal Velocity in Supercritical Circular Couette Flow". Exp. Fluids, vol. 18, pp. 1-9, 1994.

Wereley, S.T.; Lueptow, R.M. "Velocity Field for Taylor-Couette Flow with an Axial Flow". Phys Fluids, vol. 11(12), pp. 3637-3649, 1999.

Zeli Wang, Jianren Fan, Kun Luo, 2007 "Combined multi-direct forcing and immersed boundary method for simulating flows with moving particles", International Journal of Multiphase Flow 34, 283-302.

8. Responsibility notice

The authors are the only responsible for the printed material included in this paper.